Instantaneous GPS/Galileo/QZSS/SBAS Attitude Determination: A Single-Frequency (L1/E1) Robustness Analysis under Constrained Environments

N. NADARAJAH
Curtin University, Perth, Australia

P. J. G. TEUNISSEN
Curtin University, Perth, Australia
Department of Remote Sensing and Geosciences, Delft University of Technology, Delft, The Netherlands

Received August 2013; Revised December 2013

ABSTRACT: *The augmentation of new global navigation satellite systems (GNSS) to existing GPS enhances the availability of satellite based positioning, navigation, and timing (PNT) solutions. Among existing systems, the European Galileo system, the Japanese quasi-zenith satellite system (QZSS), and satellite based augmented systems (SBAS) share at least one frequency (L1/E1) with GPS. In this contribution we analyse the robustness of single-frequency instantaneous carrier-phase attitude determination using data from some or all of the four systems GPS/Galileo/QZSS/SBAS. The performance of the constrained (C)-LAMBDA method is studied under various satellite deprived environments and compared to that of the standard LAMBDA method, using L1/E1 data that was observed for ten days at Curtin University, Perth, Australia. The results demonstrate the enhanced robustness that combinations of the four systems bring to single-epoch single-frequency attitude determination. Copyright © 2014 Institute of Navigation.*

INTRODUCTION

Single-frequency positioning, navigation, and timing (PNT) using global navigation satellite systems (GNSS) is of interest for low-cost applications such as navigating unmanned aerial vehicles (UAVs). Augmenting new GNSS and regional navigation satellite systems (RNSS) to existing GPS enhances the availability of PNT solutions. Among existing systems, the European Galileo system, the Japanese quasi-zenith satellite system (QZSS), and satellite based augmentation systems (SBASs) which include the US WAAS, the European EGNOS, the Japanese MSAS, and the Indian GAGAN, share at least L1/E1 frequency with GPS. In this contribution, we analyze the robustness of pure single-frequency (L1/E1) instantaneous attitude determination under constrained environments using current constellations of the above systems.

GNSS attitude determination is a rich field of current studies, with a wide variety of challenging (terrestrial, sea, air and space) applications [1–9]. Carrier phase integer ambiguity resolution is the key to fast and high-precision GNSS positioning and attitude determination. Once this has been done successfully, the carrier phase data will act as very precise pseudo range data, thus making very precise positioning and attitude determination possible. Recent attitude determination methods make use of the popular LAMBDA method, see, e.g., [10–13], as this method is known to be efficient and known to maximize the ambiguity success rate [14–17]. However, the standard LAMBDA method has been developed for unconstrained GNSS models. The method is therefore not necessarily optimal for the GNSS attitude determination problem, for which the baseline length is often provided as well. The Constrained (C-) LAMBDA method [18–22] makes use of this information and finds the optimal nonlinear constrained integer least-squares solution. This paper demonstrates the effectiveness of the C-LAMBDA method compared to the standard LAMBDA method in resolving integer ambiguities for attitude determination using pure single-frequency observations from multi-GNSS, consisting of GPS, Galileo, QZSS, and SBAS.

Analyses of PNT solutions using a dual system (GPS with one of the other systems) have been

NAVIGATION: *Journal of The Institute of Navigation*
Vol. 61, No. 1, Spring 2014
Printed in the U.S.A.

reported in various studies. The performance of the combined GPS-Galileo PNT solutions has been analyzed in [23–27]. The benefit of augmenting GPS with QZSS is demonstrated in [28]. Beyond the intended functionality, which is to broadcast GNSS error corrections, SBAS has been proven to contribute to PNT [29–31]. In this contribution, we analyze the performance of combined four-system attitude determination using real data from identical receivers. Since intersystem biases (ISBs) [26, 32] vanish between receivers of same type [25, 29], we consider intersystem double differencing, which uses a single pivot satellite for all four systems and yields a higher level of redundancy than system-specific differencing. In the case of mixed receiver attitude determination, however, non-zero ISBs must be corrected to retain the advantage of intersystem double differencing [25].

In this contribution we concentrate on single-epoch, i.e., instantaneous, attitude determination, as this is the most challenging for integer ambiguity resolution. Moreover, when successful, it has the additional benefit of making the solutions insensitive to cycle slips. Our analyses consist of a robustness study of the C-LAMBDA method under different constrained environments, such as open-pit tracking, the presence of satellite outages, and urban canyon applications. We simulate satellite outages, open-pit masking, and the urban canyon effect using real data consisting of L1/E1 observations from GPS, Galileo, QZSS, GAGAN, and MSAS, collected for ten days at Curtin University, Perth, Australia. We analyze the corresponding performance of the C-LAMBDA method and demonstrate the enhanced robustness of multi-GNSS, single-epoch single-frequency attitude determination under such constrained environments. This study is believed to be the first four-system attitude determination analysis.

This contribution is organized as follows: *GNSS-Based Attitude Determination* describes the functional and stochastic model for GPS/Galileo/QZSS/SBAS observations. It also describes the C-LAMBDA method using the quadratically constrained GNSS model for attitude determination. *Real-Data Analysis* presents the results of attitude determination revealing improved performance of the combined system. Finally, *Conclusions* contains the summary and conclusions of this contribution.

GNSS-BASED ATTITUDE DETERMINATION

In this section we present our attitude determination method using the single frequency combined GPS/Galileo/QZSS/SBAS system. First we describe the functional and stochastic model for the combined observations and then we present the steps for solving the baseline constrained, mixed-integer attitude model.

GPS/Galileo/QZSS/SBAS Observations

Let us consider two identical GPS/Galileo/QZSS/SBAS receivers r and 1 with identical antennas forming a short baseline and collecting observations at the L1-frequency. Double differencing is used to eliminate satellite/receiver clock errors and instrumental hardware delays. When combining common frequency observations from multiple systems, one can perform either system-specific double differencing [33] or inter-system double differencing [34, 35]. In the latter case, which yields a higher level of redundancy than the former, one should, however, take into account the inter-system bias (ISB) due to system specific hardware delays, more so when mixed receiver types are used. In this work, we consider identical receivers/antennas for which ISBs are known to be absent [25, 29]. Also, since attitude determination is based on short baselines, the differential atmospheric delays can be neglected [36]. Hence, the double differenced (DD) pseudo-range and carrier-phase observations for satellite pairs 1_1-s_Φ of GNSS system pairs 1-Φ with a single pivot satellite, denoted as $p_{1r}^{1_1 s_\Phi}$ and $\phi_{1r}^{1_1 s_\Phi}$, respectively, are given as [25, 27]

$$\mathrm{E}\left(p_{1r}^{1_1 s_\Phi}\right) = \rho_{1r}^{1_1 s_\Phi},\ s_\Phi = \begin{cases} 2,\ldots,m_\Phi \text{ for } \Phi = 1 \\ 1,\ldots,m_\Phi \text{ otherwise} \end{cases} \tag{1}$$

$$\mathrm{E}\left(\phi_{1r}^{1_1 s_\Phi}\right) = \rho_{1r}^{1_1 s_\Phi} + \lambda N_{1r}^{1_1 s_\Phi}, \tag{2}$$

where $\mathrm{E}(\cdot)$ denotes the expectation operator, $\rho_{1r}^{1_1 s_\Phi}$ is the DD topocentric distance, λ is the wave length, $N_{1r}^{1_1 s_\Phi}$ is the time-invariant *integer* DD carrier-phase ambiguity, and m_Φ is the number of satellites from system Φ. For simplicity of formulation, we assume that satellites are ordered such that the first m_1 satellites are of system 1, the next m_2 satellites are of system 2, and so on $\left(\sum_{\Phi=1}^{M} m_\Phi = m+1,\right.$ the number of tracked satellites$\left.\right)$, where M is the number of systems.

The linearized DD observation equations corresponding to (1) and (2), read

$$\mathrm{E}\left(\Delta p_{1r}^{1_1 s_\Phi}\right) = g_r^{1_1 s_\Phi{}^T} b, \tag{3}$$

$$\mathrm{E}\left(\Delta \phi_{1r}^{1_1 s_\Phi}\right) = g_r^{1_1 s_\Phi{}^T} b + \lambda N_{1r}^{1_1 s_\Phi}, \tag{4}$$

where $\Delta p_{1r}^{1_1 s_\Phi}$ and $\Delta \phi_{1r}^{1_1 s_\Phi}$ are the observed-minus-computed code and phase observations, b is the baseline vector containing relative position components, and $g_r^{1_1 s_\Phi}$ is the geometry vector given as

$g_r^{1_1 s_\Phi} = e_r^{1_1} - e_r^{s_\Phi}$ with $e_r^{s_\Phi}$ the unit line-of-sight vector between receiver-satellite pair $r - s_\Phi$. The vectorial forms of the DD observation equations read

$$\mathrm{E}(y_p) \;=\; G_r b \tag{5}$$

$$\mathrm{E}(y_\phi) \;=\; G_r b + \lambda z \tag{6}$$

with

$$y_p = \left[\Delta p_{1r}^{1_1 2_1}, \ldots, \Delta p_{1r}^{1_1 m_1}, \Delta p_{1r}^{1_1 1_2}, \ldots, \Delta p_{1r}^{1_1 m_2}, \ldots, \Delta p_{1r}^{1_1 1_M}, \ldots, \Delta p_{1r}^{1_1 m_M}\right]^T \tag{7}$$

$$y_\phi = \left[\Delta \phi_{1r}^{1_1 2_1}, \ldots, \Delta \phi_{1r}^{1_1 m_1}, \Delta \phi_{1r}^{1_1 1_2}, \ldots, \Delta \phi_{1r}^{1_1 m_2}, \ldots \Delta \phi_{1r}^{1_1 1_M}, \ldots, \Delta \phi_{1r}^{1_1 m_M}\right]^T \tag{8}$$

$$G_r = \left[g_r^{1_1 2_1}, \ldots, g_r^{1_1 m_1}, g_r^{1_1 1_2}, \ldots, g_r^{1_1 m_2}, \ldots, g_r^{1_1 1_M}, \ldots, g_r^{1_1 m_M}\right]^T \tag{9}$$

$$z = \left[N_{1r}^{1_1 2_1}, \ldots, N_{1r}^{1_1 m_1}, N_{1r}^{1_1 1_2}, \ldots, N_{1r}^{1_1 m_2}, \ldots N_{1r}^{1_1 1_\eta}, \ldots, N_{1r}^{1_1 m_M}\right]^T \tag{10}$$

For the stochastic modeling (e.g., thermal noise, multipath), we apply elevation dependent weighting [37]. That is, the standard deviation of the undifferenced observable ς can be written as

$$\sigma_\varsigma(\theta) = \sigma_{\varsigma 0}\left(1 + a_{\varsigma 0} \exp\left(\frac{-\theta}{\theta_{\varsigma 0}}\right)\right) \tag{11}$$

where θ is the elevation angle of the corresponding satellite, and $\sigma_{\varsigma 0}, a_{\varsigma 0}$, and $\varepsilon_{\varsigma 0}$ are model parameters. We further assume that the receivers have similar characteristics and that the observation noise standard deviations can be decomposed as follows:

$$\begin{aligned} \sigma_{\phi_r^{s_\Phi}} &= \sigma_r \sigma_{\phi_0}^{,\Phi} \nu^{s_\Phi} \\ \sigma_{p_r^{s_\Phi}} &= \sigma_r \sigma_{p_0}^{,\Phi} \nu^{s_\Phi} \\ \nu^{s_\Phi} &= \left(1 + a_0 \exp\left(\frac{-\theta^{s_\Phi}}{\theta_0}\right)\right) \end{aligned} \tag{12}$$

where σ_r is the receiver, and $\sigma_{\phi_0}^{,\Phi}$ and $\sigma_{p_0}^{,\Phi}$ are observation dependent weightings.

The GPS/Galileo/QZSS/SBAS Constrained Baseline Model

When combining the single-epoch linearized DD GNSS code and phase observation equations of (5) and (6), we obtain the mixed integer model of observation equations:

$$\mathrm{E}(y) = Az + Gb, \;\; \begin{matrix} z \in \mathbb{Z}^m \\ b \in \mathbb{R}^3 \end{matrix} \text{ with } m = \sum_{\Phi=1}^{M} m_\Phi - 1 \tag{13}$$

where $y = \left[y_\phi^T, y_p^T\right]^T$ is the $2m \times 1$ vector of linearized (observed-minus-computed) DD carrier-phase and pseudorange observations, z is the $m \times 1$ vector of unknown DD integer ambiguities, b is a 3×1 vector of unknown baseline parameters, $G = e_2 \otimes G_r$ is the $2m \times 3$ geometry matrix with e_n the $n \times 1$ vector of 1's and $\otimes$ denoting the Kronecker product [38, 39], and $A = [\lambda I_m, 0^T]^T$ is the $2m \times m$ design matrix with I_n the identity matrix of size n.

To construct the stochastic model for the observations in (13), consider the undifferenced observations reading as

$$\zeta = \left[\zeta_1^T, \zeta_2^T\right]^T \tag{14}$$

where $\zeta_r = \left[\phi_r^T, p_r^T\right]^T$, $\phi_r = \left[\phi_r^{,1^T}, \ldots, \phi_r^{,M^T}\right]^T$, $\phi_r^{,\Phi} = \left[\phi_r^{1_\Phi}, \ldots, \phi_r^{m_\Phi}\right]^T$, $p_r = \left[p_r^{,1^T}, \ldots, p_r^{,M^T}\right]^T$, $p_r^{,\Phi} = \left[p_r^{1_\Phi}, \ldots, p_r^{m_\Phi}\right]^T$, and $p_r^{s_\Phi}$ and $\phi_r^{s_\Phi}$ are the undifferenced code and phase observations for $r - s_\Phi$ receiver-satellite pair. Using the noise characteristics of (12) and assuming the observables to be mutually uncorrelated, the dispersion matrix of the observation vector ζ can be written as

$$\mathrm{D}(\zeta) \;=\; Q_r \otimes \mathrm{blockdiag}(Q_\phi, Q_p) \tag{15}$$

where $\mathrm{D}(\cdot)$ denotes the dispersion operator, $Q_r = \mathrm{diag}\left[\sigma_1^2, \sigma_2^2\right]$, $Q_\phi = \mathrm{blockdiag}\left(Q_\phi^{,1}, \ldots, Q_\phi^{,M}\right)$, $Q_\phi^{,\Phi} = \left(\sigma_{\phi_0}^{,\Phi}\right)^2 \mathrm{diag}\left[\left(\nu^{1_\Phi}\right)^2, \ldots, \left(\nu^{m_\Phi}\right)^2\right]$, $Q_p = \mathrm{blockdiag}\left(Q_p^{,1}, \ldots, Q_p^{,M}\right)$, and $Q_p^{,\Phi} = \left(\sigma_{p_0}^{,\Phi}\right)^2 \mathrm{diag}\left[\left(\nu^{1_\Phi}\right)^2, \ldots, \left(\nu^{m_\Phi}\right)^2\right]$ are the co-factor matrices. Using the DD operator $\mathcal{D}^T = D_1^T \otimes I_2 \otimes D_m^T$, the dispersion matrix of the DD observations can be written as

$$\begin{aligned} \mathrm{D}(y) \;&=\; Q_{yy} = \mathrm{D}(\mathcal{D}^T \zeta) \\ &=\; \left(\sigma_1^2 + \sigma_2^2\right) I_2 \otimes D_m^T \mathrm{blockdiag}(Q_\phi, Q_p) I_2 \otimes D_m \end{aligned} \tag{16}$$

with $D_n^T = [-e_n, I_n]$ the differencing matrix.

The DD observation equations of (13) form, together with the dispersion matrix of (16), a *mixed-integer* Gauss-Markov model with unknown integer vector $z \in \mathbb{Z}^m$ and unknown baseline vector $b \in \mathbb{R}^3$. This model can be strengthened with the known baseline length. With the inclusion of the baseline

length constraint, we obtain the GNSS compass model [19, 20]

$$\begin{aligned} \mathrm{E}(y) &= Az + Gb \qquad \|b\| = l, z \in \mathbb{Z}^m, b \in \mathbb{R}^3 \\ \mathrm{D}(y) &= Q_{yy} \end{aligned} \tag{17}$$

where l is the known baseline length and $\|\cdot\|$ denotes the unweighted norm. Hence, the baseline is thus now constrained to lie on a sphere with radius $l (\mathbb{S}_l = \{b \in \mathbb{R}^3 \mid \|b\| = l\})$. Our objective is to solve for b in a least-squares sense, thereby taking the integer constraints on z and the quadratic constraint on vector b into account. Hence, the least-squares minimization problem that will be solved reads

$$\min_{z \in \mathbb{Z}^m, b \in \mathbb{S}_l} \|y - Az - Gb\|^2_{Q_{yy}} \tag{18}$$

with $||\cdot||^2_Q = (\cdot)^T Q^{-1} (\cdot)$. It is a quadratically constrained (mixed) integer least-squares (QC-ILS) problem [18], for which no closed-form solution is available. In the following sections, we describe the method for solving (18).

The Ambiguity Resolved Attitude

We now describe the steps for computing the integer ambiguity resolved attitude angles.

The real-valued float solution

The float solution is defined as the solution of (18) without the constraints. When we ignore the integer constraints on z and the quadratic constraint on b, the float solutions $\hat{z}$ and $\hat{b}$, and their variance-covariance matrices are obtained as follows:

$$\begin{bmatrix} Q_{\hat{z}\hat{z}} & Q_{\hat{z}\hat{b}} \\ Q_{\hat{b}\hat{z}} & Q_{\hat{b}\hat{b}} \end{bmatrix}^{-1} \cdot \begin{bmatrix} \hat{z} \\ \hat{b} \end{bmatrix} = \begin{bmatrix} A^T \\ G^T \end{bmatrix} Q_{yy}^{-1} y \tag{19}$$

with

$$\begin{bmatrix} Q_{\hat{z}\hat{z}} & Q_{\hat{z}\hat{b}} \\ Q_{\hat{b}\hat{z}} & Q_{\hat{b}\hat{b}} \end{bmatrix} = \left(\begin{bmatrix} A^T \\ G^T \end{bmatrix} Q_{yy}^{-1} [A \; G] \right)^{-1}$$

The z-constrained solution of b and its variance-covariance matrix can be obtained from the float solution as follows

$$\hat{b}(z) = \hat{b} - Q_{\hat{b}\hat{z}} Q_{\hat{z}\hat{z}}^{-1} (\hat{z} - z) \tag{20}$$

$$\begin{aligned} Q_{\hat{b}(z)\hat{b}(z)} &= Q_{\hat{b}\hat{b}} - Q_{\hat{b}\hat{z}} Q_{\hat{z}\hat{z}}^{-1} Q_{\hat{z}\hat{b}} \\ &= \left(G^T Q_{yy}^{-1} G \right)^{-1} \end{aligned} \tag{21}$$

Using the above estimators, the original problem in (18) can be decomposed as [20]

$$\min_{z \in \mathbb{Z}^m, b \in \mathbb{S}_l} \|y - Az - Gb\|^2_{Q_{yy}} =$$

$$= \|\hat{e}\|^2_{Q_{yy}} + \min_{z \in \mathbb{Z}^m} \left(\|\hat{z} - z\|^2_{Q_{\hat{z}\hat{z}}} + \min_{b \in \mathbb{S}_l} \left\| \hat{b}(z) - b \right\|^2_{Q_{\hat{b}(z)\hat{b}(z)}} \right) \tag{22}$$

with $\hat{e} = y - A\hat{z} - G\hat{b}$ being the vector of least-squares residuals. Note that the first term on the right hand side of (22) does not depend on the unknown parameters z and b and is therefore constant.

The integer ambiguity resolution

Based on the orthogonal decomposition (22), the quadratic constrained integer minimization can be formulated as:

$$\check{z} = \arg \min_{z \in \mathbb{Z}^m} C(z) \tag{23}$$

with ambiguity objective function

$$C(z) = \|\hat{z} - z\|^2_{Q_{\hat{z}\hat{z}}} + \left\| \hat{b}(z) - \check{b}(z) \right\|^2_{Q_{\hat{b}(z)\hat{b}(z)}} \tag{24}$$

where

$$\check{b}(z) = \arg \min_{b \in \mathbb{S}_l} \left\| \hat{b}(z) - b \right\|^2_{Q_{\hat{b}(z)\hat{b}(z)}} \tag{25}$$

The cost function $C(z)$ is the sum of two coupled terms: the first weighs the distance from the float ambiguity vector $\hat{z}$ to the nearest integer vector z in the metric of $Q_{\hat{z}\hat{z}}$, while the second weighs the distance from the conditional float solution $\hat{b}(z)$ to the nearest point on the sphere $\mathbb{S}_l$ in the metric of $Q_{\hat{b}(z)\hat{b}(z)}$.

Unlike with the standard LAMBDA method [40], the search space of the above minimization problem is non-ellipsoidal due to the presence of the second term in the ambiguity objective function $C(z)$. Moreover, its solution requires the computation of a nonlinear constrained least-squares problem (25) for every integer vector in the search space. In the C-LAMBDA method, this problem is mitigated through the use of easy-to-evaluate bounding functions [20, 41]. Using these bounding functions, two strategies, namely the *Expansion* and the *Search and Shrink* strategies, were developed, see, e.g., [18, 42]. These techniques avoid the computation of (25) for every integer vector in the search space, and compute the integer minimizer $\check{z}$ in an efficient manner.

The ambiguity resolved attitude

For a single baseline, b is related to the Euler-angles $\xi = [\psi, \theta]^T$, with ψ the heading and θ the elevation, as $b(\xi) = lu(\xi)$, where $u(\xi) = [c_\theta c_\psi, c_\theta s_\psi, -s_\theta]^T$ with $s_\alpha = \sin(\alpha)$ and $c_\alpha = \cos(\alpha)$. The sought-for attitude angles $\xi(\check{z})$ are the reparametrized solution of (25). Using

a first order approximation, the formal variance-covariance matrix of the ambiguity resolved, least-squares estimated heading and elevation angles is given by

$$Q_{\check{\xi}\check{\xi}} \approx \frac{1}{l^2}\left(J_{u,\xi}(\check{\xi})^T Q^{-1}_{\hat{b}(z)\hat{b}(z)} J_{u,\xi}(\check{\xi})\right)^{-1} \tag{26}$$

with Jacobian matrix

$$J_{u,\xi}(\xi) = \begin{bmatrix} -s_\psi c_\theta & -c_\psi s_\theta \\ c_\psi c_\theta & -s_\psi s_\theta \\ 0 & -c_\theta \end{bmatrix} \tag{27}$$

As the results in the next section show, this first order approximation works well. This is due to the fact that the ambiguity resolved solution is driven by the high precision of the carrier phase observables.

REAL-DATA ANALYSIS

In this section the performance analyses of GPS/Galileo/QZSS/SBAS attitude determination using real data are presented. The data was collected from two TRM59800.00-SCIS antennas mounted on the roof of the Bentley campus building 402 of Curtin University in Perth, Australia. As shown in Figure 1(a), they form a short baseline (l = 8.418 m, Figure 1(b)).

These antennas are connected to two TRIMBLE NETR9 GNSS receivers continuously tracking all available GNSS satellites. The stochastic model parameters of the elevation dependent model (11) for the receivers are reported in Table 1. The large parameter values for SBAS are due to the narrower transmitted signal bandwidth (2.2 MHz) compared to that of other systems (e.g., 20 MHz for GPS) [29, 43].

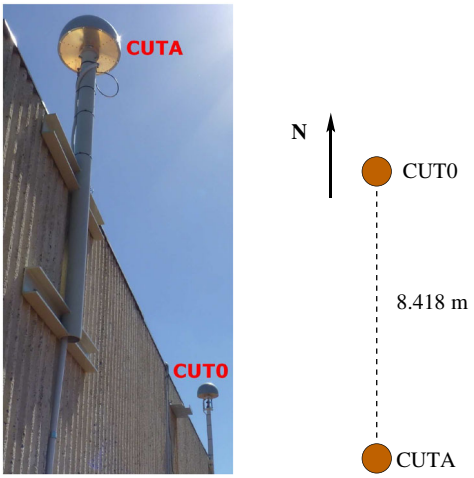

(a) Antenna setup (b) Antenna geometry

Fig. 1–Curtin GNSS antennas used for the real data campaign

Table 1 — Elevation dependent stochastic model parameters (cf., Equation (12)) for undifferenced observables with $\sigma_r = 1$ for $r = 1, 2, a_{p_0} = a_{\phi_0} = 5$ and $\varepsilon_{p_0} = \varepsilon_{\phi_0} = 20$

System (Frequency)	Code $\sigma^{\Phi}_{p_0}$ [cm]	Phase $\sigma^{\Phi}_{\phi_0}$ [mm]
GPS (L1), Galileo (E1), and QZSS (L1)	20	1
SBAS (L1)	240	7

We considered data from Curtin's stations for ten days from June 9 to 18, 2013 with a sampling interval of 30 seconds. Figure 2 shows the GPS/Galileo/QZSS/SBAS satellite visibility for June 9 (the skyplots, the number of satellites, and the PDOP values) demonstrating improved satellite visibility of the combined system.

We consider two performance measures for our analyses; the first one is the empirical instantaneous ambiguity success fraction (relative frequency), which is defined as

$$\text{success fraction} = \frac{\text{number of correctly fixed epochs}}{\text{total number of epochs}} \tag{28}$$

where the true ambiguities are computed using known antenna coordinates in WGS84 as the antennas used are part of Curtin's permanent stations. However, only length information is used for C-LAMBDA processing. The second performance measure is the ambiguity fixed angular estimation accuracy, which is given by the formal and empirical standard deviations of attitude angular estimates.

Table 2 summarizes the benefits of augmenting different systems. Augmenting GPS with one or more systems improves ambiguity resolution. Especially with C-LAMBDA, instantaneous ambiguity resolution is possible (center section, right side, values of 1.0) for the scenario considered (Figure 1). Furthermore, SBAS significantly contributes to improved ambiguity resolution even though it has less precise observations than that of other systems (Table 1). Although augmentation significantly improves ambiguity resolution and thus the ability to achieve instantaneous results, augmenting GPS with one or more systems does not significantly improve the ambiguity-fixed angular accuracy. This is understandable as any ambiguity-fixed solution is driven by the highly precise carrier-phase data. Also note that combining L1/E1-observations from non-GPS satellites does not yet offer continuous attitude solution (indicated in italicized text) due to the poor satellite geometry with current Galileo and QZSS constellations, which are under development. By combining all four systems, one can achieve instantaneous single-frequency attitude determination even with the unconstrained LAMBDA method

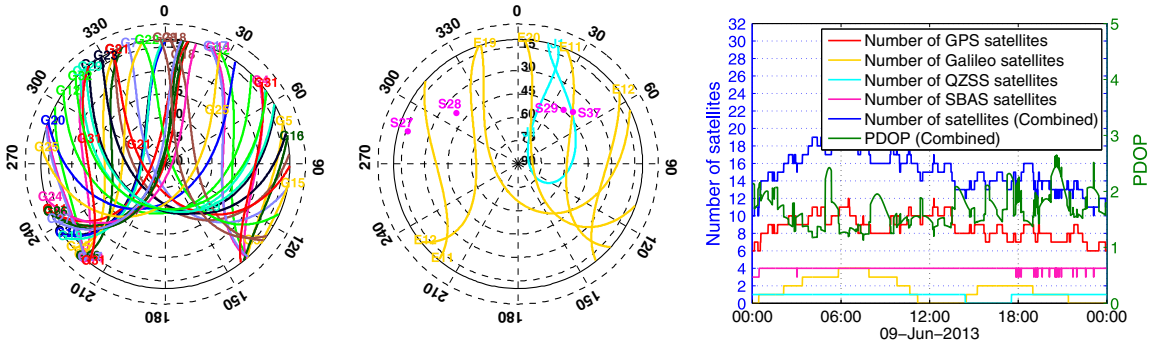

(a) Skyplot (GPS)

(b) Skyplot (Galileo: E11, E12, E19, and E20, QZSS: J1, GAGAN: S27 and S28,and MSAS: S29 and S37)

(c) Number of satellites and PDOP (Combined)

Fig. 2–Satellite visibility of GPS, Galileo, QZSS, and SBAS (GAGAN+MSAS) constellations on June 9, 2013 for 10° *elevation cut-off*

Table 2 — Instantaneous ambiguity success fractions (relative frequencies) and angular accuracy measured by empirical and formal (given in brackets) angular standard deviations. SBAS consists of two GAGAN and two MSAS satellites. For the combined Galileo/QZSS/SBAS constellation, only a fraction of epochs (given in italicized text) was processed due to the poor satellite geometry (PDOP > 100)

	Success Fraction		Angular Standard deviation [deg]	
Systems (PDOP)	LAMBDA	C-LAMBDA	Heading	Elevation
GPS (2.00)	0.85	0.99	0.01 (0.02)	0.04 (0.04)
GPS/Galileo (1.87)	0.92	1.00	0.01 (0.01)	0.03 (0.03)
GPS/QZSS (1.87)	0.94	1.00	0.01 (0.01)	0.03 (0.03)
GPS/GAGAN (1.72)	0.93	1.00	0.01 (0.02)	0.04 (0.04)
GPS/MSAS (1.87)	0.95	1.00	0.01 (0.02)	0.04 (0.04)
GPS/SBAS (1.63)	0.98	1.00	0.01 (0.01)	0.04 (0.04)
GPS/Galileo/QZSS/SBAS (1.50)	**1.00**	1.00	0.01 (0.01)	0.03 (0.03)
Galileo/QZSS/SBAS (5.75)/*0.88*	0.07	0.34	0.07 (0.07)	0.25 (0.20)

(indicated in *bold* text) for the scenario considered (Figure 1). With this clear indication of benefits from multiple system augmentation we further analyze the performance of the augmented system under various satellite deprived environments in the following sections and compare with that of GPS-only solutions.

Satellite Outages

We simulated this satellite deprived environment by arbitrarily removing a number of visible GPS satellites. Note that arbitrary removal of satellites over a long period (ten days) enables us to evaluate average performance. Table 3 reports the LAMBDA and C-LAMBDA ambiguity success fractions for single-frequency processing and ambiguity resolved attitude angular accuracy (angular standard deviation). The benefits of using C-LAMBDA are highlighted using bold text. For the scenario considered (Figure 1), the C-LAMBDA method on average offers instantaneous attitude solution with all visible satellites from current non-GPS constellations and with as few as six GPS satellites, while the LAMBDA method on average requires at least eight GPS satellites together with all visible satellites from current non-GPS constellations to achieve instantaneous solution. The formal standard deviations (terms in brackets) are well in line with the empirical standard deviations confirming the assumed stochastic model parameters in Table 1. A slight degradation of the angular accuracy with the number of satellites can be observed.

We also analyzed the contribution of the SBAS system for instantaneous attitude determination by augmenting GPS with different numbers of SBAS satellites. Table 4 summarizes the contribution of SBAS satellites highlighting the benefits of using the C-LAMBDA method (indicated using bold text). With C-LAMBDA processing, single-frequency user can achieve instantaneous attitude determination by augmenting GPS L1-observations with that of as few as one SBAS satellite for the scenario considered (Figure 1). This is an interesting boost for single-frequency users, as at least one SBAS satellite (from WAAS, EGNOS, MSAS, and GAGAN)

Table 3 — Instantaneous single-frequency ambiguity success fractions (relative frequencies) and angular accuracy measured by empirical and formal (given in brackets) angular standard deviations for simulated GPS satellite outage. For some cases, a fraction of epochs (given in emphasized text) were processed due to a poor satellite geometry for positioning (PDOP > 100)

Number of GPS	Success Fraction		Angular Standard deviation [deg]	
satellites (PDOP)	LAMBDA	C-LAMBDA	Heading	Elevation
0 (5.75)/*0.88*	0.07	0.34	0.07 (0.07)	0.25 (0.20)
2 (3.07)	0.25	0.73	0.03 (0.04)	0.08 (0.12)
4 (2.23)	0.67	0.97	0.02 (0.02)	0.06 (0.06)
6 (1.81)	0.96	**1.00**	0.02 (0.02)	0.04 (0.04)
8 (1.56)	1.00	1.00	0.01 (0.01)	0.03 (0.03)
10 (1.51)	1.00	1.00	0.01 (0.01)	0.03 (0.03)

Table 4 — The contribution SBAS: Instantaneous single-frequency ambiguity success fractions (relative frequencies) and and angular accuracy measured by empirical and formal (given in brackets) angular standard deviations for the augmentation of GPS with different number of SBAS satellites

Number of SBAS	Success Fraction		Angular Standard deviation [deg]	
satellites (PDOP)	LAMBDA	C-LAMBDA	Heading	Elevation
0 (2.00)	0.85	0.99	0.01 (0.02)	0.04 (0.04)
1 (1.92)	0.91	**1.00**	0.01 (0.02)	0.04 (0.04)
2 (1.87)	0.95	**1.00**	0.01 (0.02)	0.04 (0.04)
3 (1.81)	0.97	**1.00**	0.01 (0.01)	0.04 (0.04)
4 (1.63)	0.98	**1.00**	0.01 (0.01)	0.04 (0.04)

is uninterruptedly visible almost anywhere in the world enabling instantaneous attitude determination, which is immune to cycle slips.

Open-pit Problem

We simulated this constrained environment using elevation angle masking. Table 5 reports the ambiguity resolution success fractions for single-frequency processing with different elevation angle maskings. The benefit, improved availability of attitude solutions, of using a combined system is highlighted (in bold text).

Note that, for large elevation masking angles, a fraction of epochs (given in brackets) were processed due to a lack of sufficient visible satellites for positioning (requires at least four satellites) or due to a poor satellite geometry (PDOP > 100). For the scenario considered (Figure 1), the *single-frequency* C-LAMBDA processing of a combined system enables the availability of instantaneous attitude solutions for an open-pit with up to 20 deg elevation masking, while it is not possible for GPS-only processing even with 10 degree elevation masking.

The angular accuracies (standard deviations) of the single frequency processing are reported in

Table 5 — Instantaneous ambiguity success fractions (relative frequencies) for the real data with simulated open-pit using elevation masking; For some cases, a fraction of epochs (given in brackets) were processed due to a lack of sufficient visible satellites for positioning (requires at least four satellites) or due to a poor satellite geometry (PDOP > 100)

Elevation Cut-off	GPS only			GPS+Galileo+QZSS+SBAS		
[deg]	PDOP	LAMBDA	C-LAMBDA	PDOP	LAMBDA	C-LAMBDA
10	2.00	0.85	0.99	1.50	**1.00**	**1.00**
20	3.13	0.56	0.93	2.36	0.96	**1.00**
30	6.64 (0.94)	0.25	0.75	3.52	0.82	0.98
40	12.65 (0.65)	0.08	0.56	7.70 (0.90)	0.45	0.86
50	21.35 (0.23)	0.02	0.46	16.37 (0.26)	0.23	0.74

Table 6 — Empirical and formal (given in brackets) angular standard deviations [deg] of the ambiguity fixed attitude angles for single-frequency data with simulated open-pit using elevation masking

Elevation cut-off	GPS only		GPS+Galileo+QZSS+SBAS	
[deg]	Heading	Elevation	Heading	Elevation
10	0.01 (0.02)	0.04 (0.04)	0.01 (0.01)	0.03 (0.03)
20	0.02 (0.02)	0.04 (0.04)	0.01 (0.01)	0.04 (0.04)
30	0.02 (0.02)	0.06 (0.06)	0.02 (0.02)	0.06 (0.06)
40	0.03 (0.04)	0.11 (0.12)	0.03 (0.03)	0.11 (0.13)
50	0.04 (0.04)	0.17 (0.18)	0.03 (0.03)	0.15 (0.15)

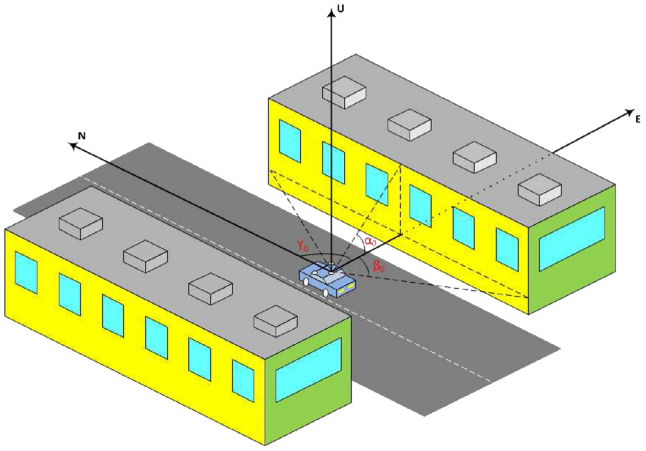

Fig. 3–Simulated urban canyon: Buildings on both sides of an urban road blocking satellite visibility; Angle γ_0 defines the direction of the road, while angles α_0 and β_0 define the height and the width of the buildings, respectively

Table 6. As shown, increasing elevation masking degrades both ambiguity resolution and the angular accuracy. But note that the combined system angular accuracy for a 20 degree mask angle is the same as that of GPS for only a 10 degree mask angle.

Urban Canyon

In this section we analyze the robustness of the C-LAMBDA method under an urban canyon effect, which is a well-known problem depriving GNSS based navigation solutions in urban environments [44–47]. We simulate the urban canyon blockage effect using a simple model, where we have two buildings as shown in Figure 3 placed symmetrically with respect to the attitude platform on an urban road. The blockage is defined by three angles: γ_0,

Table 7 — Instantaneous single-frequency ambiguity success fractions (relative frequencies) and the average computation time [sec] (given in brackets) for simulated urban canyon (Figure 3); For some cases, only a fraction of epochs (given in brackets) were processed due to the absence of sufficient satellites for positioning (requires at least four satellites) or due to a poor satellite geometry for positioning (PDOP > 100)

α_0	β_0	GPS only		GPS+Galileo+QZSS+SBAS	
(deg)	(deg)	LAMBDA	C-LAMBDA	LAMBDA	C-LAMBDA
20	20	0.80	0.99	0.99	**1.00**
	40	0.67	0.96	0.98	**1.00**
	60	0.55	0.90	0.95	**1.00**
	80	0.50 (0.99)	0.86 (0.99)	0.93	0.99
40	20	0.75	0.99	0.99	**1.00**
	40	0.43	0.85	0.93	**1.00**
	60	0.21 (0.87)	0.70 (0.87)	0.69 (0.99)	0.94 (0.99)
	80	0.14 (0.81)	0.58 (0.81)	0.58 (0.93)	0.92 (0.93)
60	20	0.72	0.98	0.99	**1.00**
	40	0.26 (0.99)	0.68 (0.99)	0.86	0.99
	60	0.03 (0.52)	0.39 (0.52)	0.17 (0.55)	0.68 (0.55)
	80	0.00 (0.13)	0.14 (0.13)	0.02 (0.14)	0.37 (0.14)
80	20	0.72	0.98	0.99	**1.00**
	40	0.23 (0.98)	0.66 (0.98)	0.83	0.98
	60	0.02 (0.45)	0.36 (0.45)	0.14 (0.46)	0.58 (0.46)
	80	0.00 (0.02)	0.27 (0.02)	0.00 (0.02)	0.40 (0.02)

Table 8 — Empirical and formal (given in brackets) angular standard deviations [deg] of the ambiguity fixed attitude angles for simulated urban canyon (Figure 3); * refers to the cases with not enough samples to compute reliable statistics

α_0	β_0	GPS only		GPS+Galileo+QZSS+SBAS	
(deg)	(deg)	Heading	Elevation	Heading	Elevation
20	20	0.02 (0.02)	0.04 (0.04)	0.01 (0.01)	0.03 (0.03)
	40	0.02 (0.02)	0.04 (0.04)	0.02 (0.02)	0.04 (0.04)
	60	0.02 (0.02)	0.04 (0.04)	0.02 (0.02)	0.04 (0.04)
	80	0.02 (0.02)	0.05 (0.04)	0.02 (0.02)	0.04 (0.04)
40	20	0.02 (0.02)	0.04 (0.04)	0.01 (0.01)	0.04 (0.03)
	40	0.02 (0.02)	0.05 (0.06)	0.02 (0.02)	0.05 (0.05)
	60	0.03 (0.03)	0.05 (0.06)	0.03 (0.03)	0.05 (0.05)
	80	0.03 (0.03)	0.06 (0.06)	0.03 (0.03)	0.05 (0.05)
60	20	0.02 (0.02)	0.04 (0.04)	0.01 (0.01)	0.04 (0.04)
	40	0.02 (0.02)	0.06 (0.07)	0.02 (0.02)	0.05 (0.05)
	60	0.09 (0.10)	0.10 (0.11)	0.07 (0.07)	0.08 (0.08)
	80	* (*)	* (*)	* (*)	* (*)
80	20	0.02 (0.02)	0.04 (0.04)	0.01 (0.01)	0.04 (0.04)
	40	0.02 (0.03)	0.07 (0.07)	0.02 (0.02)	0.05 (0.06)
	60	0.10 (0.11)	0.12 (0.12)	0.08 (0.08)	0.10 (0.10)
	80	* (*)	* (*)	* (*)	* (*)

the azimuth of the center of the first building (defining the direction of the road), α_0, the elevation at the center of the building (defining the height of the buildings), and β_0, the azimuth angle (defining the width of the buildings). For example, in the case of $\gamma_0 = 90°, \alpha_0 = 60°$, and $\beta_0 = 60°$, the model represents two buildings with a height of 9 meters and a width of 17 meters on both sides of a ten-meter wide road in the North-South direction. Urban canyons can also introduce multi-path effects [46] and sometimes other types of interference [48] that are not considered in this contribution. The robustness of the C-LAMBDA method against multi-path effects has already been studied and demonstrated in [49, 50] using a simulation study.

We considered the urban canyon along a road in the North-South direction ($\gamma_0 = 90°$). This corresponds to the worst case deprivation due to a lack of visible satellites towards the South direction in Perth, Australia (South polar region). Table 7 summarizes the ambiguity resolution success fraction for the simulated urban canyon scenario demonstrating the benefits (highlighted using bold text) of augmenting systems. Note that, for large values of α_0 and β_0, only a fraction of epochs (given in brackets) were processed due to the absence of sufficient satellites for positioning (requires at least four satellites) or due to a poor satellite geometry (PDOP > 100). For almost all other cases of combined system with the scenario considered (Figure 1), instantaneous ambiguity resolution is possible due to the exploitation of the geometry constraints in the C-LAMBDA method. The corresponding angular accuracies (standard deviations) are reported in Table 8, showing that empirical values are in line with formal values (given in brackets). A combined system processing not only improves the success fraction, but also slightly improves the angular accuracies. Both the ambiguity resolution success fraction and the angular accuracy, however, degrade as the effect of the urban canyon increases (i.e., angles α_0 and β_0 increase).

CONCLUSIONS

In this article we analyzed the performance of the C-LAMBDA method for instantaneous attitude determination using single-frequency (L1/E1) observations from GPS/Galileo/QZSS/SBAS. Using real data from a rooftop experiment, we demonstrated that through any of the given augmentations of GPS, instantaneous single-frequency attitude determination is achieved with the C-LAMBDA method. We also demonstrated that such is even possible with the unconstrained LAMBDA method, at least in the Asia-Pacific region, when all four systems are combined in a mild multipath environment. We further analyzed the performance of single-frequency attitude determination under various satellite deprived environments. The C-LAMBDA method offers instantaneous attitude solution with all visible satellites from current non-GPS constellations and with as few as six GPS satellites, while the LAMBDA method requires at least eight GPS

satellites together with all visible satellites from current non-GPS constellations to achieve instantaneous solution.

The *single-frequency* C-LAMBDA processing of a combined system enables the availability of instantaneous attitude solutions for an open-pit with up to 20 degree elevation masking, while this is not possible for GPS-only processing even with 10 degree elevation masking. We also showed that the use of a combined constellation significantly improves the attitude solution availability under the satellite masking effect in an urban environment. Overall, this study demonstrated the realization of instantaneous attitude determination by combining single-frequency (L1/E1) observations from all available systems in a mild multipath environment.

ACKNOWLEDGMENTS

This work has been executed in the framework of the Positioning Program Project 1.01, "New carrier phase processing strategies for achieving precise and reliable multi-satellite, multi-frequency GNSS/RNSS positioning in Australia" of the Cooperative Research Centre for Spatial Information (CRC-SI) and the Australian Space Research Program GARADA project on SAR Formation Flying. The second author P. J. G. Teunissen is the recipient of an Australian Research Council Federation Fellowship (project number FF0883188). All this support is gratefully acknowledged.

REFERENCES

1. Lu, G., "Development of a GPS Multi-Antenna System for Attitude Determination," Ph.D. Dissertation, Department of Geomatics Engineering, University of Calgary, Calgary, Alberta, Canada, 1995.
2. Tu, C.-H., Tu, K., Chang, F.-R., and Wang, L.-S., "GPS Compass: A Novel Navigation Equipment," *IEEE Transactions on Aerospace and Electronic Systems*, Vol. 33, No. 3, July 1997, pp. 1063–1068.
3. Bar-Itzhack, I.Y., Montgomery, P. Y., and Garrick, J. C., "Algorithm for attitude determination using GPS," *Proceedings of AIAA Guidance, Navigation, and Control Conference*, New Orleans, LA, August 1997, pp. 841–851.
4. Bell, T., "Error Analysis of Attitude Measurement in Robotic Ground Vehicle Position Determination," *NAVIGATION*, Vol. 47, No. 4, Winter 2000, pp. 289–296.
5. Caporali, A., "Basic Direction Sensing with GPS," *GPS World*, Vol. 12, No. 3, 2001, pp. 44–50.
6. Park, K. J., and Crassidis, J. L., "Attitude Determination Methods Using Pseudolite Signal Phase Measurements," *NAVIGATION*, Vol. 53, No. 2, Summer 2006, pp. 121–133.
7. Pinchin, J., Hide, C., Park, D., and Chen, X., "Precise Kinematic Positioning Using Single Frequency GPS Receivers and an Integer Ambiguity Constraint," *Position, Location and Navigation Symposium, 2008 IEEE/ION*, Monterey, CA, May 2008, pp. 600–605.
8. Jurkowski, P., Henkel, P., and Guenther, C., "GPS Based Attitude Determination with Statistical and Deterministic Baseline a priori Information," *Proceedings of the 2012 International Technical Meeting of The Institute of Navigation*, Newport Beach, CA, January 2012, pp. 1164–1213.
9. Chiang, K. Q., Psiaki, M. L., Powell, S. P., Miceli, R. J., and O'Hanlon, B. W., "GPS-Based Attitude Determination for a Spinning Rocket," *Proceedings of the 25th International Technical Meeting of the Satellite Division of The Institute of Navigation (ION GNSS 2012)*, Nashille, TN, September 2012, pp. 2342–2350.
10. Furuno, Model SC-120: Satellite compass. Available from: http://www.furunousa.com/products/default.aspx, 2003, [Online; accessed: 28-March-2013].
11. Monikes, R., Wendel, J., and Trommer, G. F., "A Modified LAMBDA Method for Ambiguity Resolution in the Presence of Position Domain Constraints," *Proceedings of the 18th International Technical Meeting of the Satellite Division of The Institute of Navigation (ION GNSS 2005)*, Long Beach, CA, September 2005, pp. 81–87.
12. Kuylen, L. V., Nemry, P., Simsky, A., and Lorga, J., "Comparison of Attitude Performance for Multi-Antenna Receivers," *European Journal of Navigation*, Vol. 4, No. 2, May 2006, pp. 1–9.
13. Wang, B., Miao, L., Wang, S., and Shen, J., "A Constrained LAMBDA Method for GPS Attitude Determination," *GPS Solutions*, Vol. 13, No. 2, March 2009, pp. 97–107.
14. Teunissen, P. J. G., De Jonge, P., and Tiberius, C., "Performance of the LAMBDA Method for Fast GPS Ambiguity Resolution," *NAVIGATION*, Vol. 44, No. 3, Fall 1997, pp. 373–400.
15. Teunissen, P. J. G., "An Optimality Property of the Integer Least-Squares Estimator," *Journal of Geodesy*, Vol. 73, 1999, pp. 587–593.
16. Cox, D. B., and Brading, J. D. W., "Integration of LAMBDA Ambiguity Resolution with Kalman Filter for Relative Navigation of Spacecraft," *NAVIGATION*, Vol. 47, No. 3, Fall 2000, pp. 205–210.
17. Verhagen, S., and Teunissen, P. J. G., "New Global Navigation Satellite System Ambiguity Resolution Method Compared to Existing Approaches," *Journal of Guidance, Control, and Dynamics*, Vol. 29, No. 4, 2006, pp. 981–991.
18. Park, C., and Teunissen, P. J. G., "A New Carrier Phase Ambiguity Estimation for GNSS Attitude Determination Systems," *Proceedings of International Symposium on GPS/GNSS*, Tokyo, Japan, November 2003, pp. 283–290.
19. Teunissen, P. J. G., "The LAMBDA Method for the GNSS Compass," *Artificial Satellites*, Vol. 41, No. 3, 2006, pp. 89–103.
20. Teunissen, P. J. G., "Integer Last-squares Theory for the GNSS Compass," *Journal of Geodesy*, Vol. 84, No. 7, 2010, pp. 433–447.
21. Teunissen, P. J. G., Giorgi, G., and Buist, P. J., "Testing of a New Single-Frequency GNSS Carrier Phase Attitude Determination Method: Land, Ship and Aircraft Experiments," *GPS Solutions*, Vol. 15, No. 1, 2011, pp. 15–28.
22. Giorgi, G., Teunissen, P. J. G., Verhagen, S., and Buist, P. J., "Testing a New Multivariate GNSS Carrier Phase Attitude Determination Method for Remote Sensing Platforms," *Advances in Space Research*, Vol. 46, No. 2, 2010, pp. 118–129.

23. Hahn, J., and Powers, E., "GPS and Galileo Timing Interoperability," *Proceedings of GNSS 2004*, Rotterdam, the Netherlands, May 2004, pp. 1–5.
24. Bonhoure, B., Boulanger, C., and Marechal, J., "Long Term and Multi-Receiver GPS/GIOVE Mixed PVT Experimentation," *Proceedings of the 23rd International Technical Meeting of the Satellite Division of The Institute of Navigation (ION GNSS 2010)*, Portland, OR, September 2010, pp. 3309–3319.
25. Odijk, D., and Teunissen, P., "Characterization of Between-Receiver GPS-Galileo Inter-System Biases and their Effect on Mixed Ambiguity Resolution," *GPS Solutions*, Vol. 17, No. 4, October 2013, pp. 521–533.
26. Odijk, D., Teunissen, P. J. G., and Huisman, L., "First Results of Mixed GPS+GIOVE Single-Frequency RTK in Australia," *Journal of Spatial Sciences*, Vol. 57, No. 1, June 2012, pp. 3–18.
27. Nadarajah, N., Teunissen, P. J. G., and Raziq, N., "Instantaneous GPS-Galileo Attitude Determination: Single-Frequency Performance in Satellite-Deprived Environments," *IEEE Transactions on Vehicular Technology*, Vol. 62, No. 7, 2013, pp. 2963–2976.
28. Wu, F., Kubo, N., and Yasuda, A., "Performance Evaluation of GPS Augmentation using Quasi-Zenith Satellite System," *IEEE Transactions on Aerospace and Electronic Systems*, Vol. 40, No. 4, 2004, pp. 1249–1260.
29. Wanninger, L., and Wallstab-Freitag, S., "Combined Processing of GPS, GLONASS, and SBAS Code Phase and Carrier Phase Measurements," *Proceedings of the 20th International Technical Meeting of the Satellite Division of The Institute of Navigation (ION GNSS 2007)*, Fortworth, TX, September 2007, pp. 866–875.
30. Boriskin, A., Kozlov, D., and Zyryanov, G., "L1 RTK System with Fixed Ambiguity: What SBAS Ranging Brings," *Proceedings of the 20th International Technical Meeting of the Satellite Division of The Institute of Navigation (ION GNSS 2007)*, Fortworth, TX, September 2007, pp. 2196–2201.
31. Wanninger, L., "The Future is Now - GPS + GLONASS + SBAS = GNSS," *GPS World*, July 2008, pp. 42–48.
32. Dach, R., Lutz, S., Meindl, M., Schaer, S., Steigenberger, P., and Beutler, G., "Combining the Observations from Different GNSS," *Proceedings of EUREF 2010 Symposium*, Gävle, Sweden, June 2010, pp. 1–5.
33. Verhagen, S., and Joosten, P., "Algorithms for Design Computations for Integrated GPS-Galileo," *Proceedings of the European Navigation Conference*, (ENC-GNSS'03), Graz, Austria, April 2003, pp. 1–14.
34. Julien, O., Alves, P., Cannon, M. E., and Zhang, W., "A Tightly Coupled GPS/GALILEO Combination for Improved Ambiguity Resolution," *Proceedings of the European Navigation Conference*, (ENC-GNSS'03), Graz, Austria, April 2003, pp. 1–14.
35. Julien, O., Cannon, M., Alves, P., and Lachapelle, G., "Triple Frequency Ambiguity Resolution using GPS/Galileo," *European Journal of Navigation*, Vol. 2, No. 2, 2004, pp. 51–57.
36. Teunissen, P. J. G., and Kleusberg, A., *GPS for Geodesy*, 2nd ed, Berlin; New York: Springer, 1998.
37. Euler, H.-J., and Goad, C., "On Optimal Filtering of GPS Dual Frequency Observations without using Orbit Information," *Journal of Geodesy*, Vol. 65, 1991, pp. 130–143.
38. Harville, D. A., *Matrix Algebra From A Statisticians Perspective*, New York: Springer, 1997.
39. Magnus, J. R., and Neudecker, H., *Matrix Differential Calculus with Applications in Statistics and Econometrics*, New York: Wiley, 1995.
40. Teunissen, P. J. G., "The Least-Squares Ambiguity Decorrelation Adjustment: A Method for Fast GPS Integer Ambiguity Estimation," *Journal of Geodesy*, Vol. 70, 1995, pp. 65–82.
41. Nadarajah, N., Teunissen, P. J. G., and Giorgi, G., "GNSS Attitude Determination for Remote Sensing: On the Bounding of the Multivariate Ambiguity Objective Function," in *Earth on the Edge: Science for a Sustainable Planet, International Association of Geodesy Symposia*, Rizos, C. & Willis, P., eds., Springer, Berlin Heidelberg, 2014, Vol. 139, pp. 503–509.
42. Giorgi, G., Teunissen, P. J. G., and Buist, P. J., "A Search and Shrink Approach for the Baseline Constrained LAMBDA Method: Experimental Results," in *Proceedings of International Symposium on GPS/GNSS*, Tokyo, Japan, November 2008, pp. 797–806.
43. Phelts, R. E., Walter, T., Enge, P., Akos, D. M., Shallberg, K., and Morrissey, T., "Range Biases on the WAAS Geostationary Satellites," *Proceedings of the 2004 National Technical Meeting of The Institute of Navigation*, San Diego, CA, January 2004, pp. 110–120.
44. Tsakiri, M., Stewart, M., Forward, T., Sandison, D., and Walker, J., "Urban Fleet Monitoring with GPS and GLONASS," *The Journal of Navigation*, Vol. 51, No. 03, 1998, pp. 382–393.
45. Ballester-Grpide, I., Herriz-Monseco, E., Juez-Muoz, A., Romay-Merino, M. M., and Beech, T. W., "Future GNSS Constellation Performances Inside Urban Environments," *Proceedings of the 13th International Technical Meeting of the Satellite Division of The Institute of Navigation (ION GPS 2000)*, Salt Lake City, UT, September 2000, pp. 2436–2445.
46. Aloi, D., and Korniyenko, O., "Comparative Performance Analysis of a Kalman Filter and a Modified Double Exponential Filter for GPS-Only Position Estimation of Automotive Platforms in an Urban-Canyon Environment," *IEEE Transactions on Vehicular Technology*, Vol. 56, No. 5, September 2007, pp. 2880–2892.
47. Ji, S., Chen, W., Ding, X., Chen, Y., Zhao, C., and Hu, C., "Potential Benefits of GPS/GLONASS/Galileo Integration in an Urban Canyon - Hong Kong," *The Journal of Navigation*, Vol. 63, No. 04, 2010, pp. 681–693.
48. Bertran, E., and Delgado-Penin, J., "On the Use of GPS Receivers in Railway Environments," *IEEE Transactions on Vehicular Technology*, Vol. 53, No. 5, September 2004, pp. 1452–1460.
49. Giorgi, G., "GNSS Carrier Phase-Based Attitude Determination Estimation and Applications," Ph.D. Dissertation, Delft University of Technology, December 2011.
50. Nadarajah, N., and Teunissen, P. J. G., "Instantaneous GPS/BeiDou/Galileo Attitude Determination: A Single-Frequency Robustness Analysis under Constrained Environments," *Proceedings of The Institute of Navigation Pacific PNT 2013*, Honolulu, Hawaii, April 2013, pp. 1088–1103.